Physica C: Superconductivity and its applications 588 (2021) 1353929

Contents lists available at ScienceDirect

Physica C: Superconductivity and its applications

journal homepage: www.elsevier.com/locate/physc

Sample capacity and anvil size effects for a standardized method to determine the delamination strength of 2G HTS coated conductors

Ce Sun [a,b,c], Cong Liu [a,b,c], Xingyi Zhang [a,b,c,*], Youhe Zhou [a,b,c]

[a] Institute of Superconductor Mechanics, Lanzhou University, Gansu, 730000,China
[b] Key Laboratory of Mechanics on Disaster and Environment in Western China attached to the Ministry of Education of China, Lanzhou University, Lanzhou, Gansu, 730000,China
[c] Department of Mechanics and Engineering Sciences, College of Civil Engineering and Mechanics, Lanzhou University, Lanzhou, Gansu, 730000,China

ARTICLE INFO

Keywords:
Mechanical delamination strength (MDS)
HTS CCs
Weibull distribution
Sample capacity
Anvil size

ABSTRACT

Anvil tests are effective for determination of the mechanical delamination strength (MDS) of 2G high temperature superconducting coated conductors (CCs), which has been widely used. However, the discrete property of measurement data makes the MDS of CCs hard to evaluate just from the average and variance. To properly provide an analysis of these discrete experimental data, the three-parameter Weibull distribution analysis along with its reliability function has been adopted, from the criterion of 99% reliability, the obtained MDS is conveniently referred for both engineering test and design. Nevertheless, the stable and reliable Weibull distribution analysis should be based on enough sample capacity and proper anvil size. In this work, the influences of anvil size and sample capacity on the reliability function of Weibull distribution analysis for MDS determination were systematically investigated at 77K. It is found that the minimum of sample capacities for Weibull distribution analysis are different with different anvil sizes. From the aspects of energy dissipation and cost consumption, we recommend the full width size of anvils to be utilized to obtain the justified MDS of CCs without being slitted.

1. Introduction

Second generation of high temperature superconducting coated conductors (2G HTS CCs), with high current density, high critical temperature and high irreversible magnetic field, are becoming widely used for various applications in the large-scale power industry, such as the high-field magnets, energy storages and transmission cables, etc. [1-3]. In contrast with the round Nb_3Sn wires and multi-filamentary Bi-based HTS tapes, the CCs are more susceptible to the applied transverse tensile stresses because of their unique composited multi-layer structure, which is still a main problem hindering their application in extreme environments under thermal stresses [4,5] and Lorentz forces [6-9]. It has been found serious degradation of critical current (I_c) took place in either epoxy impregnated coil during cooling down [10] or paraffin impregnated coil after charging in a strong background magnetic field [7], and delamination is one of the important reasons that caused serious degradation of critical current on CCs. From the aspect view of mechanics, transverse mechanical strength of CCs plays an important role on the reliability of both multilayer structure and electromagnetic behavior. Hence it is significant to measure the transverse mechanical strength of CCs. For a CC sample, the brittle ceramic layers including ReBCO layer and buffer layer are together sandwiched by the ductile metal layers, i.e. silver, copper and substrate layers. For the reason that the fracture toughness of the metal layer, in the order of kJ/m^2 [11], is several orders higher than the ceramic layer, typically in the order of J/m^2 [12], the whole CC sample can be regarded as a mechanical structure that the metal layers are jointed together by these ceramic adhesives. As a result, the bonding strength in the transverse direction is mainly determined by the cohesive bonding strength in the matrix of each ceramic layer itself and adhesive strength between the interfaces [13]. In order to achieve a better understanding of the mechanical properties of this "joint" structure, especially the stress response along the transverse direction, testing methods are classified into four types based on the exerted stress types [14]. The first is c-axis tensile test, such as anvil [15-29], pin-pull [30] and three point bending tension tests [31]. The stress is featured as being applied perpendicular to the CC surface. The delamination strength is obtained as the ratio of the peak tensile force to the exerted area. The second contains cleavage [32-35]

* Corresponding author.
E-mail address: zhangxingyi@lzu.edu.cn (X. Zhang).

https://doi.org/10.1016/j.physc.2021.1353929
Received 4 November 2020; Received in revised form 9 May 2021; Accepted 11 July 2021
Available online 15 July 2021

Table 1
Specification of YBCO CCs samples.

Sample	Width	Fabricationprocess	Structure	Stabilizer	Manufacturer
YBCO SCS6050	6 mm width	IBAD/MOCVD	Ag(2μm) YBCO (1μm) Hastelloy (50μm)	Copper (20μm)	Superpower
ST-10-E	10 mm width	IBAD/PLD	Ag(2μm) YBCO (1μm) Hastelloy (50μm)	Copper (5μm)	Shanghai ST

and peel [12,13,36] methods, Cleavage is defined as the stress occurring when forces at one end of a rigid bonded assembly act to pry the adherends apart. Using the double cantilever assembly, the fracture toughness *G* was acquired [32,34,35]. Peeling is similar to the cleavage, but it applies to a joint where one or both of the adherends are flexible. Though the peel test with a fixed angle, T-peel test, and climbing drum peel test, the peeling force per unit width was achieved [13,36], as well as the derived fracture toughness G [12], but there should be noted that peeling results strongly depend on the peeling angle and the energy contribution from macroscopic plastic, e.g. the results rely on the thickness of copper stabilizer. The last kind is attributed to the environmental tests, including delamination measurement by thermal stress, from which the temperature dependence of fracture toughness K_{IC} was first measured [37] and coil degradation experiments, in which the delamination strength was just a function of the ratio between the outer and inner diameters [38-40]. Though various types of approaches are presented, no method has been found, so far, can be applied universally, it is still important to select the correct method for particular case under investigation [41-43]. On this point, a simple, efficient and practical method should be provided to test the transverse mechanical strength by considering both the mechanical and electrical behavior. Among these methods, anvil method is easy to implement and is the only approach existed that can carry the superconducting current during the test. The anvil method was first adopted by *van der Laan et al.* [15] to evaluate the transverse mechanical delamination strength (MDS) for CCs. *Shin et al.* [19] gave the definition of mechanical delamination and electro-mechanical delamination, and conducted a series systematic works on factors that influence the anvil measurements. For mechanical delamination test, it was found that the slitting process in fabrication reduced the measured MDS due to the crack formation of superconducting layer near the cut edge of the CC samples [15,17,18,24,25,28]. Though the anvil measurement is not influenced by the factors, like contact configuration [23,28], loading speed [21] and thickness of the silver layer [29], all delamination strength data show a high degree of dispersion [16,17,19,21-29,44], the dispersion degree depends on the anvil size [17,19,24], and the position in the CC with cut edge [17,23,25]. The micro analyses [19,23,30], through scanning electron microscope (SEM), energy disperse spectroscopy (EDS) or optical microscope, reveal the delamination occurs in the forms of both intralaminar fracture of ceramic matrix and interlaminar crack at interface. Hence the brittle fractures make the discrete data hard to evaluate just through the average and variance. For this reason, a Weibull distribution analysis is employed to make an efficient analysis [19,21,25,44]. In our previous work [44], a criterion based on the Weibull reliability function was provided and the corresponding mechanical and electromechanical delamination strengths are reasonable and can be used as a reference for the engineering test and design. Nevertheless, the number of sample capacity and optimum anvil size for a proper Weibull distribution statistics are still not concerned in previous researches. In this paper, the MDS of CC sample at 77K was studied with anvil method. We focused on two problems, the one is the sample capacity, explaining how many of the samples used could provide the stable and reasonable reliability function; the other is, for a sample with integrated width without being silted, how big the size of the anvil is efficient to acquire the proper delamination strength along c-axis. The solving of two problems are expected to be useful for making anvil testing approach as a standard method for engineering testing and evaluating MDS during the practical application.

2. Experimental procedure

2.1. Samples

The YBCO CCs used for this study were ST-10-E from Shanghai Superconductor Technology Co., Ltd (Shanghai ST) and SCS 6050 from SuperPower. The YBCO layers were deposited by the IBAD-PLD and IBAD-MOCVD techniques, respectively. The width of samples for Shanghai ST is 10 mm, and that for SuperPower is 6 mm. It is noted that

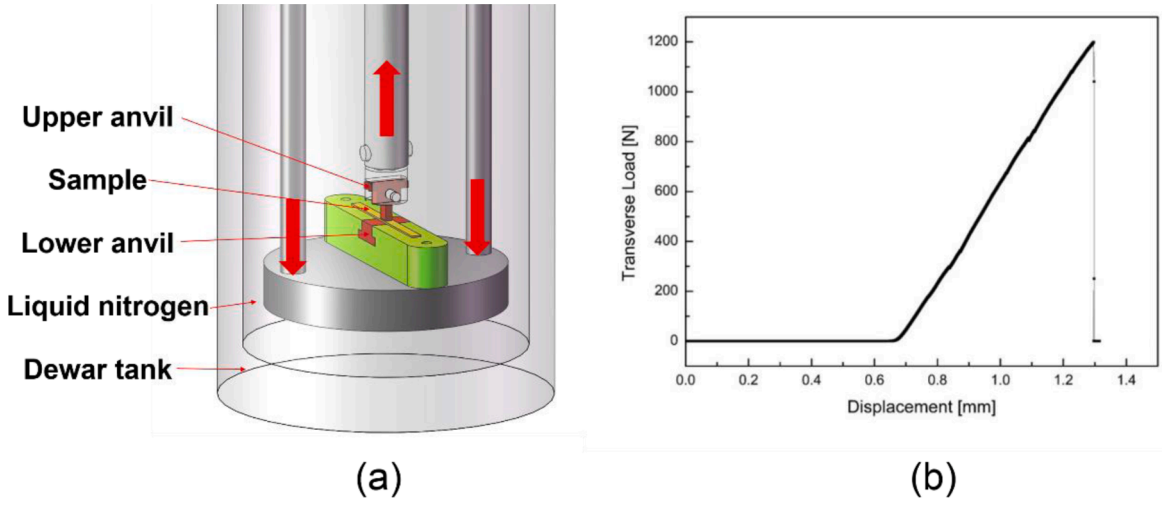

Fig. 1. (a) Loading assembly for delamination test under 77K, below which a Dewar tank with liquid nitrogen was added. (b) Load-displacement curves obtained under transverse tensile loads with the speed of 0.1 mm/min and the curves defined the MDS of CCs.

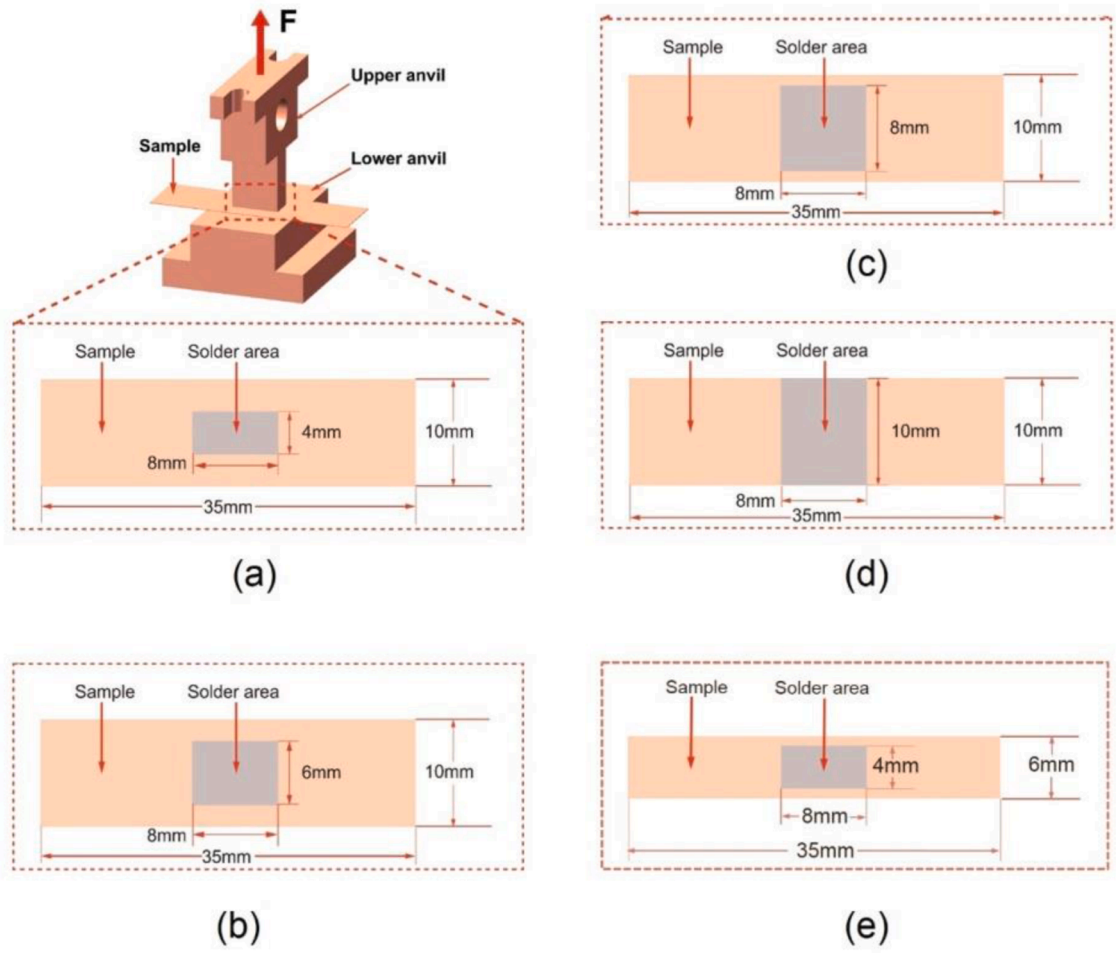

Fig. 2. The upper anvils with different widths of 4 mm, 6 mm, 8 mm and 10 mm and the soldered areas on the 10 mm wide CCs samples made from Shanghai ST are (a) 4 × 8 mm, (b) 6 × 8 mm, (c) 8 × 8 mm and (d) 10 × 8 mm. (e) The upper anvils with the width of 4 mm and the soldered areas on the 6 mm wide CCs samples made from SuperPower is 4 × 8 mm.

all the samples from Shanghai ST were cut from the same piece of CC in length, and the width of the whole piece of CC is intact that without slitted. Hence the damage effects due to the slitting process on the measurements were not considered in this case. Table 1 shows the specification of samples used in this study.

2.2. Experimental assembly and system

Before soldering, oxide layers on the surfaces of upper and lower anvils were removed by sandpaper with average particle diameter of 15.3μm, and then M705 solder manufactured by the Senju Metal Industry Company with the melting point of 220°C was filled on the surfaces of anvils and sample. Next, the sample, upper and lower anvils were kept aligned by homemade welding supporting fixture as in our last work [44], the whole soldering assembly was placed on the heating platform until solder is well melted, and the temperature of the platform was kept to 230 °C for 5 minutes and the sample was soldered together with the upper and lower anvils, so that no bending moments would be induced on the sample surface during tension. After that, the soldered entirety of anvils and sample cooled down naturally, and was then taken out from the supporting fixture and assembled in universal material testing machine. In the loading assembly, the upper anvil was connected with upper loading rod by a plug, and the lower anvil was inserted into a G-10 base of glass epoxy that was fixed with the lower loading frame, shown in Fig. 1(a).

In the MDS test the displacement is controlled at a ramp rate of 0.1 mm/min. The MDSs were acquired when a sudden drop of load from the force–displacement curve occurred, as shown in Fig. 1(b).

The MDS is defined as

$$\sigma = \frac{F_{\max}}{S}, \tag{1}$$

where $F_{\max}$ is the maximum force in the force–displacement curve, S is the soldering area.

To investigate the effect of loading area size on the measurement of the delamination strength of CCs, anvils with different widths were employed, shown in Fig. 2. The widths of the upper anvils used in this experiment are 4 mm, 6 mm mm, 8 mm, and 10 mm, and with same length of 8 mm, respectively. The 10 × 8 mm anvil which has an area of 80 mm^2 covers the whole width of the CCs.

3. Results and discussion

3.1. Weibull analysis for discrete MDSs of YBCO CCs

The measured data of the MDSs of YBCO CCs using anvils with different sizes at 77K are plotted in Fig. 3. For each upper anvil size, the corresponding maximum, minimum, average and variance of the MDSs are summarized in the Table 2. From the Table 2, one can find the average values seem to be larger with narrower anvils. Most importantly, all the measurement results show dispersed properties and depend on the anvil size, the nearly same magnitude of average and

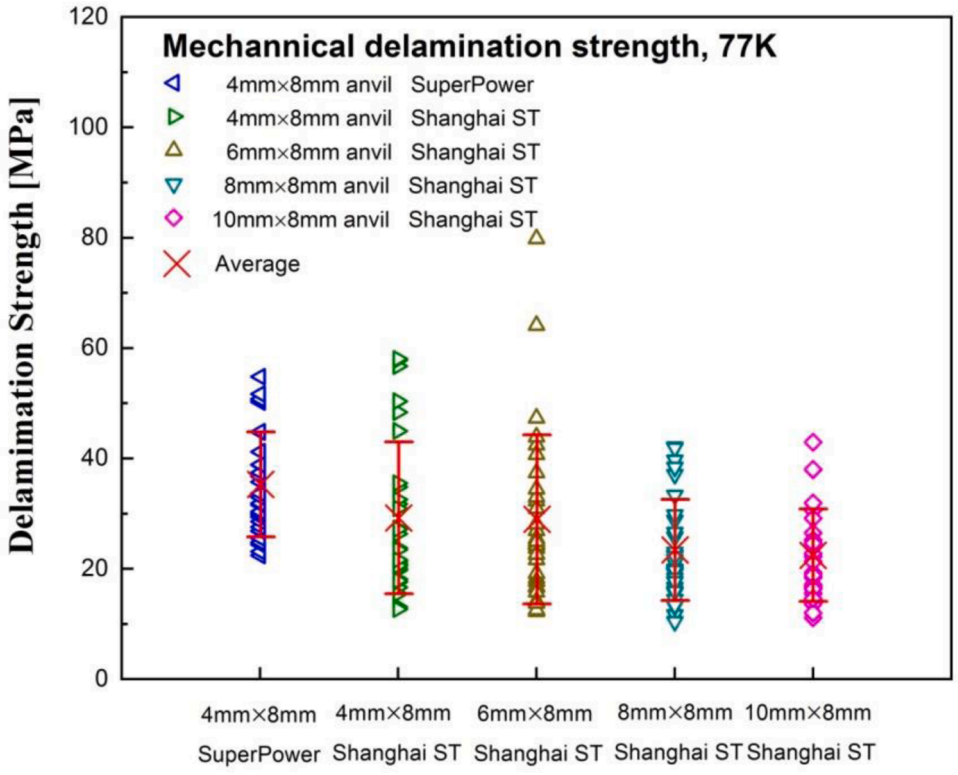

Fig. 3. The MDSs of YBCO CCs using different upper size anvils.

Table 2
The statistic MDS results with different upper anvil sizes.

	Maximum strength(MPa)	Minimum strength(MPa)	Averagestrength(MPa)	Standard deviation(MPa)	Sample capacity
4 × 8 mm Shanghai ST, 77K	58	12.7	29.2	13.8	29
6 × 8 mm Shanghai ST, 77K	79.8	12.3	28.9	15.4	30
8 × 8 mm Shanghai ST, 77K	42.1	10.4	23.3	9.2	30
10 × 8 mm Shanghai ST, 77K	42.9	11.1	22.4	8.4	25
4 × 8 mm SuperPower, 77K	54.8	22.5	35.3	9.5	30

variance values make it hard to evaluate the stability and reliability of both the experimental method and system. Considering delamination in the CC is in the form of the fracture of ceramic layers, i.e. interlaminar fracture due to adhesive de-bonding and intralaminar fracture because of cohesive de-bonding, hence discrete distribution is the intrinsic properties in fractures of these ceramic constituent layers.

The Weibull-distribution method works as an efficient tool to describe the discrete properties of the MDS of CCs, as it is successfully give a reasonable statistics for brittle fractures for ceramic materials. Here three-parameter Weibull distribution function is used and expressed as:

$$F(x;\alpha,\beta,\gamma) = 1 - \exp\left\{ - [(x-\gamma)/\alpha]^{\beta} \right\}, \quad (2)$$

where x is variable and α, β and γ are the scale, shape, and location parameters. The detail to determine the parameters of α, β and γ, as well as their physical meanings can be found in our previous work [44].

3.2. The applicability of the weibull distribution analysis for the MDS of CCs by different fabrication processes

The Weibull plots of the MDSs of YBCO CCs from Shanghai ST at 77K using different sizes of anvils are displayed in Fig. 4 (a)-(d) and CCs from SuperPower is plotted in Fig. 4(e). Fig. 5 plots the reliability as a function of the transverse tensile stress, the black line represents the mechanical reliability of YBCO CCs from Shanghai ST using 4 × 8 mm upper anvil and the blue line represents the case of mechanical reliability of YBCO CCs from SuperPower using 4 × 8 mm upper anvil. According to this diagram, when the reliability of transverse tensile stress is 99%, the corresponding tensile stress are 12.13 MPa and 22.00 MPa for the CCs from Shanghai ST and SuperPower, respectively. One can find that the Weibull distribution method is effective to describe the MDSs of CCs by different fabrication processes, which indicates that Weibull distribution statistical analysis is universal to describe the MDSs of different types of CCs.

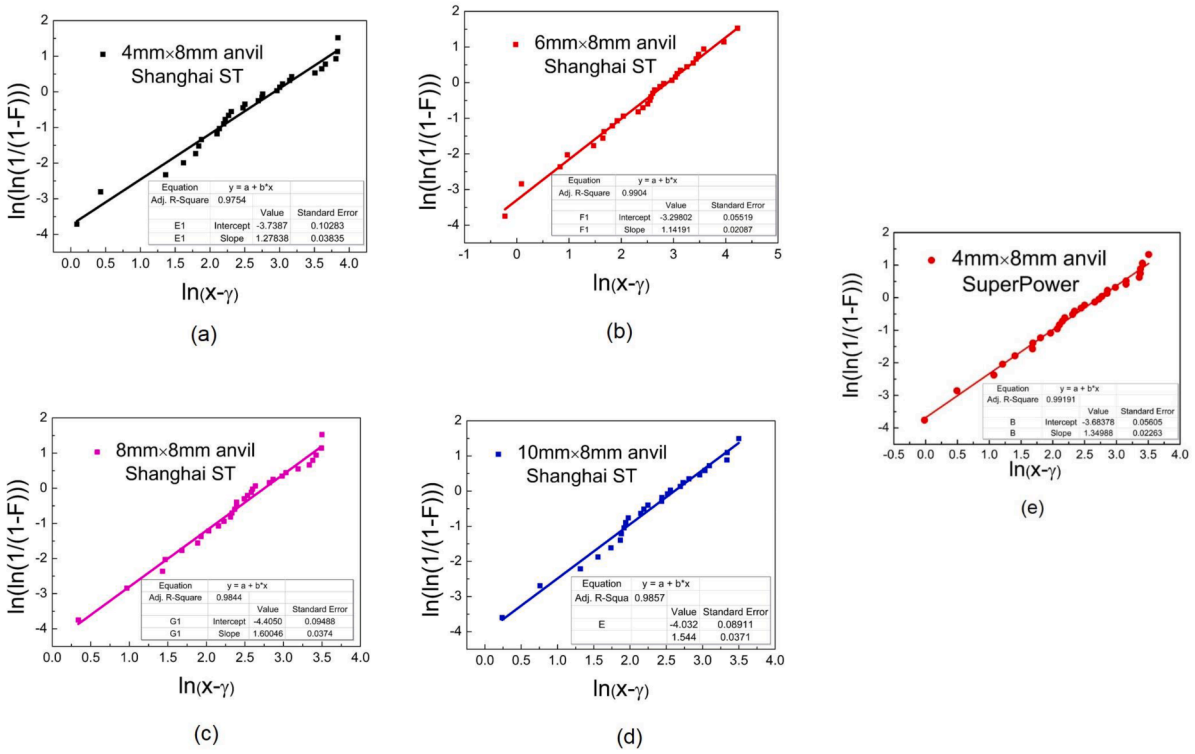

Fig. 4. The three-parameter Weibull distribution of the MDSs of YBCO CCs from Shanghai ST measured with different sizes of upper anvils at 77K: (a) 4 × 8 mm upper anvil, (b) 6 × 8 mm upper anvil, (c) 8 × 8 mm upper anvil and (d) 10 × 8 mm upper anvil. (e) The three-parameter Weibull distribution of the MDSs of YBCO CCs from SuperPower measured with 4 × 8 mm upper anvil at 77K.

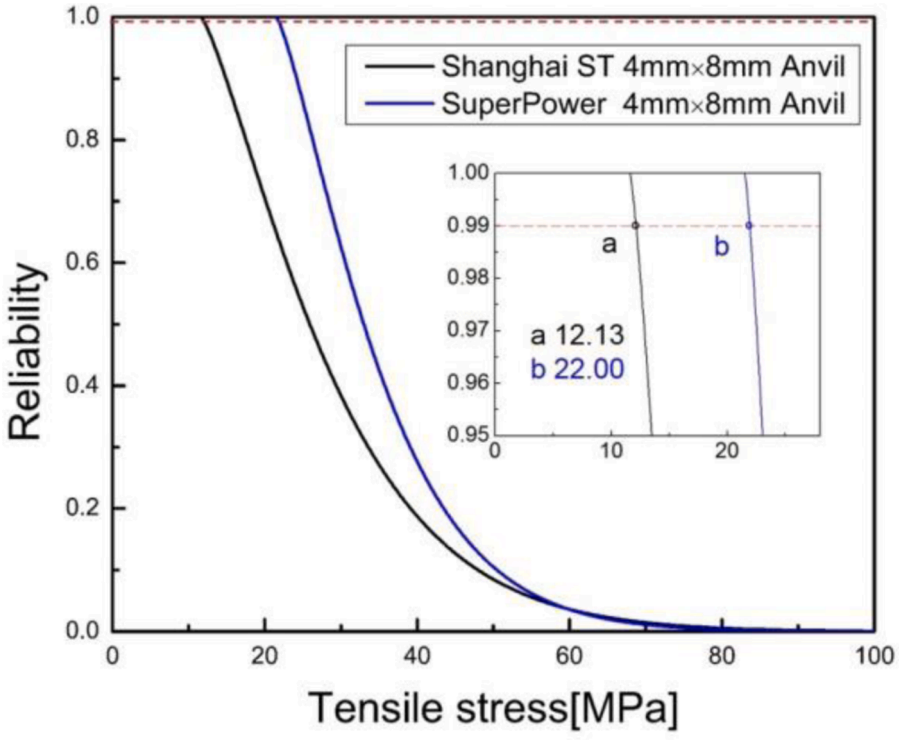

Fig. 5. The reliability of MDS as a function of tensile stress, the inset shows the MDSs determined from the criterion of 99% reliability, the value for Shanghai ST is 12.13 MPa and for SuperPower is 22.00 MPa.

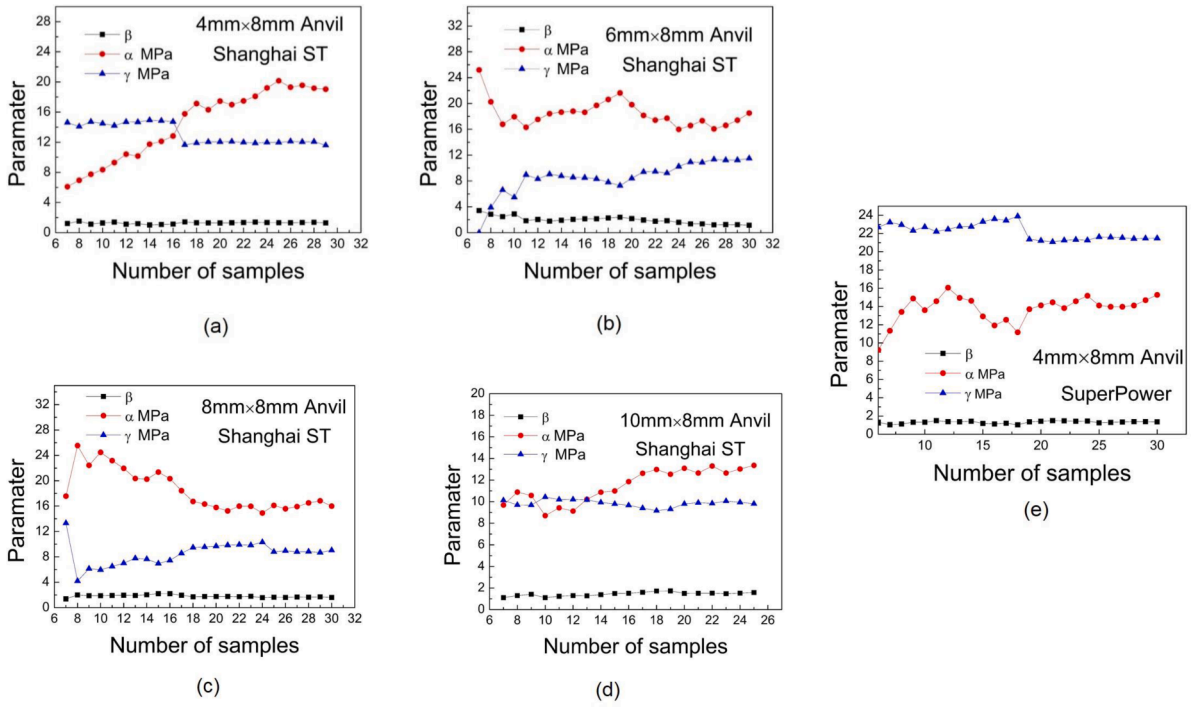

Fig. 6. The three parameters estimated from different sample capacity with different anvil sizes, samples were made from Shanghai ST: (a) 4 × 8 mm upper anvil, (b) 6 × 8 mm upper anvil, (c) 8 × 8 mm upper anvil and (d) 10 × 8 mm upper anvil. (e) The three parameters estimated with anvil size of 4 × 8 mm upper anvil from samples made form SuperPower Inc. at 77K.

Table 3
The sample capacity and MDSs with different upper anvil sizes at 77K.

Sample capacity	SuperPower 4 × 8 mm Anvil (MPa)	Shanghai ST 4 × 8 mm Anvil (MPa)	Shanghai ST 6 × 8 mm Anvil (MPa)	Shanghai ST 8 × 8 mm Anvil (MPa)	Shanghai ST 10 × 8 mm Anvil (MPa)
8	23.17	14.43	7.90	6.75	10.01
9	22.76	14.86	9.22	8.08	10.10
10	23.12	14.72	9.12	8.10	10.57
11	22.87	14.56	10.32	8.62	10.43
12	23.64	14.88	10.13	9.10	10.47
13	23.76	14.90	10.44	9.63	10.44
14	23.35	15.07	10.47	9.76	10.32
15	23.57	15.03	10.54	9.61	10.30
16	23.80	14.97	10.69	9.97	10.23
17	23.70	12.28	10.63	10.32	10.12
18	24.02	12.41	10.54	10.61	10.05
19	21.82	12.52	10.44	10.73	10.19
20	21.78	12.53	10.80	10.86	10.41
21	21.74	12.60	11.11	10.98	10.51
22	21.86	12.57	10.74	11.02	10.49
23	21.9	12.54	10.70	11.06	10.61
24	21.89	12.59	11.12	11.12	10.58
25	21.98	12.60	11.48	9.76	10.55
26	21.99	12.70	11.45	9.86	-
27	21.98	12.69	11.71	9.83	-
28	21.96	12.73	11.66	9.85	-
29	21.98	12.13	11.66	9.82	-
30	22.00	-	11.82	9.94	-

3.3. The determination of minimum sample capacity for Weibull distribution analysis of MDS

The parameters for Weibull distribution of MDS with different sample capacities are shown in Fig. 6. It can be found that the estimated parameters vary with the different sample capacities, but gradually converged and eventually tend to be stable with the increase of sample capacity. To quantitatively determine the minimum sample capacity, it is implemented as followed. The MDS is obtained with reliability of R=99% expressed as

$$x = \alpha_n \left[\ln\left(\frac{1}{99\%}\right)\right]^{\frac{1}{\beta_n}} + \gamma_n. \tag{3}$$

where α_n, β_n, and γ_n, are parameters when the sample capacity is n. The MDS data with different sample capacities are shown in Table 3.

We consider the parameters with the max sample capacity in each experimental test as a reference, the correspondence parameters are α_m, β_m, and γ_m. The difference between the acquired MDSs with other sample capacities and the reference one is expressed as:

Table 4
The minimum sample capacities for different CCs and anvil sizes

	SuperPower 4 × 8 mm Anvil	Shanghai ST 4 × 8 mm Anvil	Shanghai ST 6 × 8 mm Anvil	Shanghai ST 8 × 8 mm Anvil	Shanghai ST 10 × 8 mm Anvil
±5% of the MDSs(MPa)	20.90~23.10	11.52~12.74	11.23~12.41	9.44~10.44	10.02~11.08
Minimum sample capacity	19	17	25	25	9

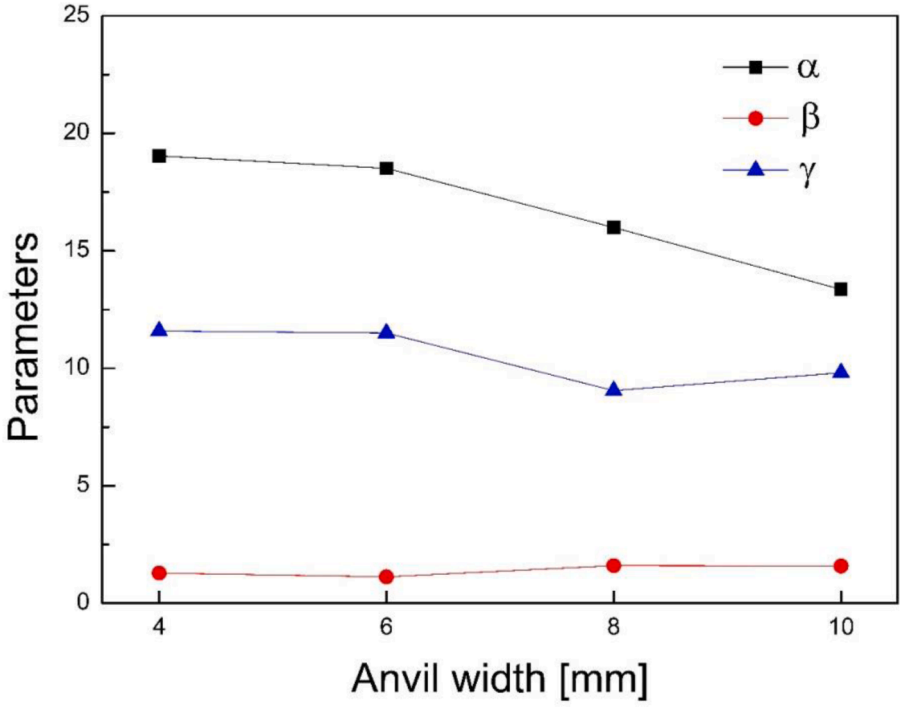

Fig. 7. The parameters of the Weibull distribution function estimated form results of different widths of anvils.

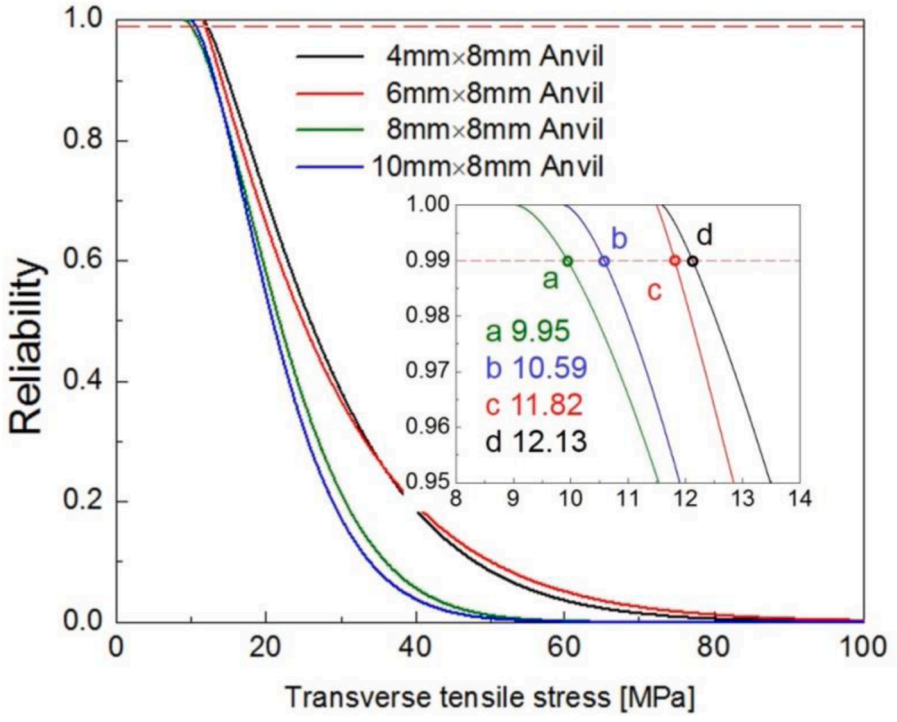

Fig. 8. The reliability of MDS as a function of tensile stress, the inset shows the MDSs determined from the criterion of 99% reliability, the value for 4 × 8 mm upper anvil is 12.13 MPa, . for 6 × 8 mm upper anvil is 11.82 MPa. for 8 × 8 mm upper anvil is 9.95 MPa and for 10 × 8 mm upper anvil is 10.59 MPa.

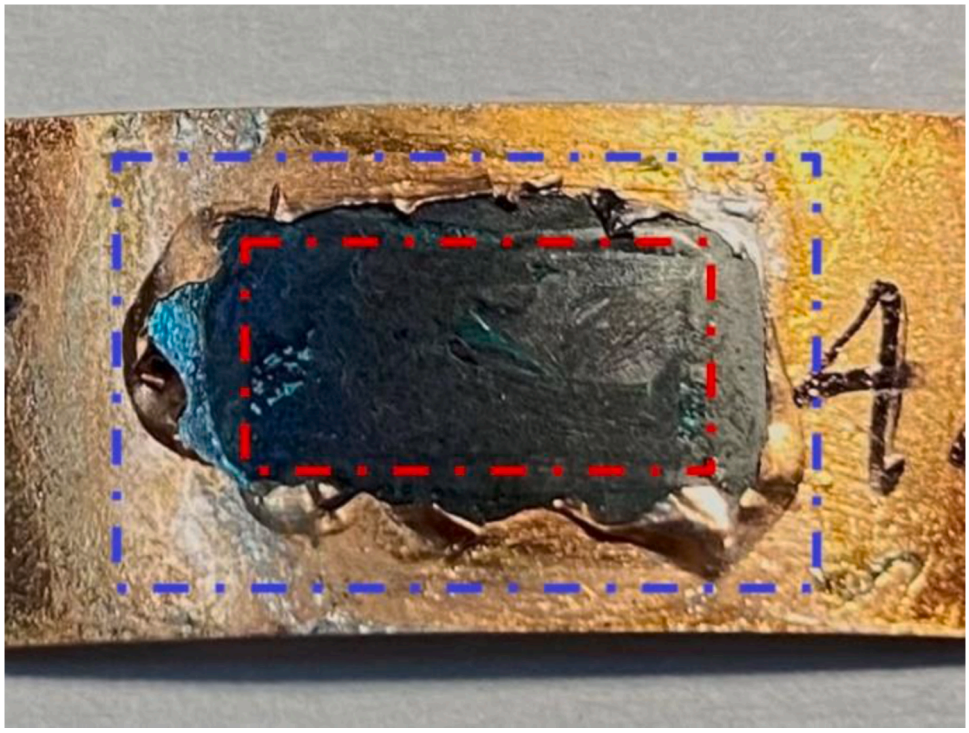

Fig. 9. Plastic deformation of the stabilizer layer at the edge of solder area

$$x\big|_{\alpha_n,\beta_n,\gamma_n} - x\big|_{\alpha_m,\beta_m,\gamma_m} = \left((\alpha_n-\alpha_m)\frac{\partial}{\partial\alpha} + (\beta_n-\beta_m)\frac{\partial}{\partial\beta} + (\gamma_n-\gamma_m)\frac{\partial}{\partial\gamma}\right)x\big|_{\alpha_m,\beta_m,\gamma_m}$$
$$+\frac{1}{2!}\left((\alpha_n-\alpha_m)\frac{\partial}{\partial\alpha} + (\beta_n-\beta_m)\frac{\partial}{\partial\beta} + (\gamma_n-\gamma_m)\frac{\partial}{\partial\gamma}\right)^2 x\big|_{\alpha_m,\beta_m,\gamma_m}$$
$$+\cdots+\frac{1}{p!}\left((\alpha_n-\alpha_m)\frac{\partial}{\partial\alpha} + (\beta_n-\beta_m)\frac{\partial}{\partial\beta} + (\gamma_n-\gamma_m)\frac{\partial}{\partial\gamma}\right)^p x\big|_{\alpha_m,\beta_m,\gamma_m} \tag{4}$$

Eqn 6

One can see the contribution of parameter difference, α_n-α_m, β_n-β_m and γ_n- γ_m, to the error is coupled in the higher order terms. Therefore we take the derived MDS x with α_m, β_m, and γ_m as a reference, which is thought to be close to the true value, then define the ±5% of the MDS reference as a criterion. At last the minimum sample capacities for different anvil sizes are determined if the calculated MDS data falls into this range, as displayed in Table 4. From the dataset of Table 4, it is found the test of full width size anvil needs as smallest as 9 among all anvil sizes.

3.4. Anvil size dependence of MDS

Using the maximum of sample capacity, the Weibull plots of the MDSs of YBCO CCs at 77K for different anvil sizes are displayed in Fig. 4 (a)-(d), and the anvil size dependence of parameters are plotted in Fig. 7.

It is found that the shape parameter β basically does not change with the increase of the width of anvil, indicating the failure rate in different conditions are nearly the same. The scale parameter α manifests there are a wide distribution of delamination strength with small anvil size and a narrow distribution with big anvil size, illustrating that with the increase of the width of anvil, the distribution of delamination strength is more concentrated, similar behavior can also be found in works [19,21,24]. Compared to the width of anvil are 8 mm and 10 mm (close to the width of the YBCO CCs), the γ are higher when the anvil are narrower (4 mm and 6 mm).

From the Fig. 8, the results with wide anvils sizes of 8 × 8 mm and 10 × 8 mm derived from the criterion of 99% reliability are 9.95 MPa and 10.59 MPa, respectively. Two values are almost equal, and are smaller than the results with narrow anvil sizes of 4 × 8 mm with 12.13 MPa and 6 × 8 mm with 11.82 MPa, the trend of anvil size dependence of MDS is consistent with other works [17,19,24].

To explain the little difference of MDSs from different anvil sizes, here we provide a qualitative analysis in terms of energy. For anvil tensile test, we define

$$W_{experimental} = \int \sigma A dl = G_0 + G_1, \tag{5}$$

where $W_{experimental}$ is the work of universal testing machine, σ is tensile stress, A is calculate area, l is the displacement of the upper anvil, G_0 is the energy dissipation of the delamination at solder area, marked by red rectangle in Fig. 9, containing energy of adhesive de-bonding and cohesive de-bonding, and G_1 is the energy dissipation including stabilizer plastic deformation and extra peel near the edge of solder, the area between the blue and red marked rectangles. Ideally, the delamination strength is just dependent on G_0, nevertheless, G_1 is inevitable during the test, and we consider the G_0 dominates if the larger width of upper anvil is used. This is because G_0 is in proportion to the solder area S while G_1 is in proportion to the perimeter of the anvil. For example, in the Fig. 2(a) and Fig. 2(c), the areas of the 4 mm width anvil and 8 mm width anvil are equal to 32 mm^2 and 64 mm^2, respectively. The area of 8 mm width anvil is double of the 4 mm width anvil, in contrast, the circumference of the 4 mm width anvil is 24 mm and 32 mm for the 8 mm width anvil, which is less than double. If we use the anvil of full width size the G_1 can be minimized (in this scenario, no plastic deformation of copper and extra peel exist at double edges along the length direction of CC sample), result in the most reasonable MDS result in the measurement. Therefore, the larger size of anvil used, the smaller contribution of the G_1 is acquired, anvils with width completely cover the width of the CCs is recommended to determine the MDS in the Weibull distribution analysis.

4. Conclusions

The mechanical delamination strengths (MDSs) of CCs at 77K were

systematically measured by anvils with different sizes. From these, we can conclude the followings: (1) the example of the MDSs for CC samples fabricated by different processing technologies was given to show the present Weibull analysis available. (2) From the criterion provided, there exists minimum sample capacity for each group measurement under a given anvil size, which is significant to provide a justified Weibull distribution analysis. (3) Qualitative energy analysis suggests the MDS test with full width size of anvil provides the value close to the intrinsic MDS of CCs. For these reasons, the full width size of anvils is recommended for determination of the MDSs of 2G HTS CCs from Weibull distribution analysis. (4) If we consider the parameters with the max sample capacity in case of the full width size as a reference, and then define the ±5% of the MDS reference as a criterion, it is found that the test of full width size anvil needs only 9, which can reach the expected criterion.

Declaration of Competing Interest

None.

Acknowledgements

This work is supported by the Fund of Natural Science Foundation of China (No.11902130, 11872196). All the authors thank Shanghai Superconductor Technology Co., Ltd (Shanghai ST) for the free samples. These experimental data presented here are only used to characterize our experimental and data processing methods. The performance of the samples is not evaluated in this paper.

References

[1] D. Hazelton, Y. Xie, V. Selvamanickam, R. Anthony, J.C. Llambes, T. Lehner, in Innovative Technologies for An Efficient & Reliable Electricity, Supply (2010).
[2] J. Schwartz, et al., IEEE Trans. Appl. Supercond. 18 (2008) 70.
[3] D. Larbalestier, A. Gurevich, M. Feldmann, A. Polyanskii, Nature 414 (2001) 368.
[4] H. Miyazaki, S. Iwai, T. Tosaka, K. Tasaki, Y. Ishii, IEEE Trans. Appl. Supercond. (2014) 24.
[5] H. Miyazaki, S. Iwai, T. Tosaka, K. Tasaki, Y. Ishii, IEEE Trans. Appl. Supercond. (2015) 25.
[6] C. Senatore, M. Alessandrini, A. Lucarelli, R. Tediosi, D. Uglietti, Y. Iwasa, Cheminform (2014) 47.
[7] K. Kajita, et al., IEEE Trans. Appl. Supercond. 26 (2016) 1.
[8] T. Matsuda, T. Okamura, M. Hamada, S. Matsumoto, T. Ueno, R. Piao, Y. Yanagisawa, H. Maeda, Cryogenics 90 (2018) 47.
[9] S. Hahn, et al., Nature 570 (2019) 496.
[10] T. Takematsu, R. Hu, T. Takao, Y. Yanagisawa, H. Nakagome, D. Uglietti, T. Kiyoshi, M. Takahashi, H. Maeda, Physica C: Superconductivity & Its Applications 470 (2010) 674.
[11] Y. Wei, J.W. Hutchinson, Int. J. Fract. 95 (1999) 1.
[12] N.J. Long, R.C. Mataira, E. Talantsev, R.A. Badcock, IEEE Trans. Appl. Supercond. 28 (2018) 1.
[13] I. Kesgin, N. Khatri, Y. Liu, L. Delgado, E. Galstyan, V. Selvamanickam, Supercond. Sci. Technol. 29 (2015), 015003.
[14] E.M. Petrie, Handbook of Adhesives and Sealants, McGraw-Hill, 2000.
[15] D.C. van der Laan, J. Ekin, C.C. Clickner, T.C. Stauffer, Supercond. Sci. Technol. 20 (2007) 765.
[16] H. Jeong, S. Kim, I.K. Yu, S. Lee, K. Sim, H.S. Ha, S.S. Oh, S.H. Moon, IEEE Trans. Appl. Supercond. 22 (2012), 7700804.
[17] H. Park, H. Jung, S. Kim, M. Park, S. Lee, H.-s. Ha, S.-H. Moon, S. Jeong, IEEE Trans. Appl. Supercond. 23 (2012), 6602504.
[18] A. Gorospe, A. Nisay, J. Dizon, H. Shin, Physica C: Superconductivity & Its Applications 494 (2013) 163.
[19] H.S. Shin, A. Gorospe, Supercond. Sci. Technol. 27 (2014) 2.
[20] X. Zhang, W. Liu, J. Zhou, Y.-H. Zhou, Rev. Sci. Instrum. 85 (2014), 125115.
[21] A.B. Gorospe, Z.M. Bautista, H.-S. Shin, Progr. Superconduct. Cryogen. 17 (2015) 13.
[22] A. Gorospe, A. Nisay, H.S. Shin, Physica C 504 (2014) 47.
[23] A. Gorospe, M.J. Dedicatoria, H.-S. Shin, IEEE Trans. Appl. Supercond. 25 (2014) 1.
[24] H.-S. Shin, A.B. Gorospe, M.J. Dedicatoria, Rev. Sci. Instrum. 86 (2015), 106112.
[25] A. Gorospe, M.J. Dedicatoria, H.-S. Shin, IEEE Trans. Appl. Supercond. 26 (2016) 1.
[26] Z.M. Bautista, H.-S. Shin, IEEE Trans. Appl. Supercond. 29 (2019) 1.
[27] J. Wang, C. Sun, L. Cong, X. Zhang, Y. Zhou, Theor. Appl. Mech. Lett. 9 (2019) 147.
[28] H.-S. Shin, Supercond. Sci. Technol. 32 (2019), 104001.
[29] M.A. Diaz, H.-S. Shin, H. Ha, S.-S. Oh, Progr. Superconduct. Cryogen. 21 (2019) 34.
[30] G. Majkic, E. Galstyan, Y. Zhang, V. Selvamanickam, IEEE Trans. Appl. Supercond. 23 (2013), 6600205.
[31] P. Jin, J. Liu, J. Liu, L. Li, J. Cheng, X. Li, Q. Wang, IEEE Trans. Appl. Supercond. 28 (2017) 1.
[32] N. Sakai, S. Lee, N. Chikumoto, T. Izumi, K. Tanabe, Physica C 471 (2011) 1075.
[33] Y. Yanagisawa, H. Nakagome, T. Takematsu, T. Takao, N. Sato, M. Takahashi, H. Maeda, Physica C 471 (2011) 480.
[34] T. Miyazato, M. Hojo, M. Sugano, T. Adachi, Y. Inoue, K. Shikimachi, N. Hirano, S. Nagaya, Physica C 471 (2011) 1071.
[35] M. Hojo, Y. Tanie, M. Sugano, Y. Inoue, M. Nishikawa, K. Shikimachi, T. Watanabe, N. Hirano, S. Nagaya, Physics Procedia 27 (2012) 252.
[36] Y. Zhang, et al., Physica C 473 (2012) 41.
[37] K. Suzuki, M. Tomita, Phyisica C: Superconductivity & Its Applications 470 (2010) 1342.
[38] H. Miyazaki, S. Iwai, T. Tosaka, K. Tasaki, Y. Ishii, IEEE Trans. Appl. Supercond. 24 (2013) 1.
[39] H. Miyazaki, S. Iwai, T. Tosaka, K. Tasaki, Y. Ishii, IEEE Trans. Appl. Supercond. 25 (2015) 1.
[40] S. Muto, S. Fujita, K. Akashi, T. Yoshida, Y. Iijima, K. Naoe, IEEE Trans. Appl. Supercond. (2018) 1.
[41] R. Jacobsson, Thin Solid Films 34 (1976) 191.
[42] T.R. Hull, J.S. Colligon, A.E. Hill, Vacuum 37 (1987) 327.
[43] P.A. Steinmann, H.E. Hintermann, J. Vacuum Sci. Technol. 7 (1989) 2267.
[44] X.Y. Zhang, C. Sun, C.L. Liu, Y.H. Zhou, Supercond. Sci. Technol. (2020) 33.